

Temperature dependence of the probability for scattering of charge carriers in molybdenum and tungsten

V. V. Boiko, V. F. Gantmakher, and V. A. Gasparov

Institute of Solid State Physics, USSR Academy of Sciences

(Submitted April 12, 1973)

Zh. Eksp. Teor. Fiz. 65, 1219–1226 (September 1973)

Experimental information on the probability of carrier scattering by various sections of the Fermi surface of molybdenum and tungsten is obtained in investigations of the temperature dependences of the radio-frequency size-effect line amplitudes carried out in the 1.5–12°K range. The temperature-dependent part of the collision frequency for molybdenum is found to be proportional to T^2 up to 12°K. A quadratic dependence is observed in tungsten only below about 6°K; a T^3 law is observed above this temperature. An attempt is made to analyze the possible contribution of electron-electron scattering to the observed temperature dependences. On the basis of available information on the electron spectra of molybdenum and tungsten and on the shape of their Fermi surfaces, a comparison is carried out with nontransition metals.

INTRODUCTION

Numerous measurements of the resistivity of pure metals at low temperatures can be summarized in the following manner.

In nontransition metals, the resistance varies with temperature in most cases in accordance with the law $\rho = \rho_0 + bT^5$. The deviations from this law have been fairly well investigated. They are most frequently connected with the freezing out of the umklapp processes^[1] or the processes of "intervalley" electron-phonon scattering from one section of the Fermi surface to another, and also with singularities of the topology of the Fermi surface^[2], with interference of scattering by impurities and phonons^[3], and with the influence of the crystal surface^[4]. These deviations, however, are all relatively small, and it is usually assumed that the temperature-dependent part of the resistance is due to electron-phonon scattering.

In transition metals, the picture is essentially different. If we disregard different complicating circumstances of the type noted above, then we can state that at low temperatures in pure transition metals we have the relation $\rho - \rho_0 = aT^2 + bT^5$ (see, e.g.,^[5,6], where there are extensive references to earlier investigations). The quadratic term in $\rho(T)$ is usually attributed to electron-electron scattering, since it is known that the frequency of the electron-electron collisions is proportional to T^2 ^[7].

The explanation as to why these collisions appear in transition metals and do not appear in nontransition metals is usually based on Mott's two-band model of transition metals^[8]. This model presupposes the presence of two parabolic unfilled bands: one with an effective mass and velocity close to the corresponding values for free electrons (electronic s-band), and another with a high density of states and correspondingly heavy mass and small velocity on the Fermi surface (heavy d band). In this model, it is the light carriers that are responsible for the charge transport, and the heavy carriers make a small contribution to the current, but serve as scattering centers for the light ones.

It seems to us, however, and we shall attempt to demonstrate this below, that there are not sufficient grounds for contrasting tungsten and molybdenum with nontransition metals on the basis of this model, and that a different explanation should be sought for the observed quadratic dependence of $\rho(T)$. By way of a first step in

this direction, we have undertaken measurements of the temperature dependence of the scattering probability for different groups of carriers (situated in different sections of the Fermi surface) in tungsten and molybdenum, using for this purpose the radiofrequency size effect.

As is well known, the size-effect lines are formed by a relatively narrow layer of orbits on the Fermi surface, located near the orbit with extremal dimension, and the amplitude of the line is proportional to the number of electrons from this layer traversing the path from one side of the plate to the other without scattering. Therefore the temperature dependence of each individual line yields information on the scattering of the electrons from the states along the corresponding extremal orbit.

The size effect has been used many times to study scattering by phonons in nontransition metals. The measured quantity ν_{ph} turns out to be proportional here to T^3 , and not to T^5 , inasmuch as in the size effect one measures the total collision frequency rather than the transport collision frequency, whose reciprocal ν_{ph}^{-1} is the average time between two elementary acts of collision with phonons^[9,10].

The results of analogous measurements for tungsten and molybdenum will be described in the next section.

EXPERIMENT

Measurements of the amplitude of the size-effect lines were carried out by plotting the derivatives $\partial R/\partial H$ and $\partial^2 R/\partial H^2$ of the real part of the surface impedance with respect to the magnetic field in the frequency range 0.8–8 MHz and in the temperature interval 1.5–12°K. The setup and the measurement procedure, and also the methods used to vary and to measure the temperature and to prepare the samples are described in^[10–12]. The purity of the initial single-crystal ingots from which the samples were made was characterized by the ratio $\rho(293^\circ\text{K})/\rho(4.2^\circ\text{K}) \approx 1.8 \times 10^4$ for molybdenum and $\sim 3.5 \times 10^4$ for tungsten.

If the electron has time to execute only half a revolution along its trajectory during the free-path time, then the line amplitude A is connected with the temperature-dependent part of the effective collision frequency $\nu(T)$ by a formula which is very convenient for the measurements, namely $A \propto \exp(-\pi\nu/\Omega)$ at $\nu + \nu_0 > \Omega$, where ν_0 is the frequency of the collisions with the static defects, $\Omega = eH/mc$ is the cyclotron frequency, and e and m are the charge and cyclotron mass of the electron, while c

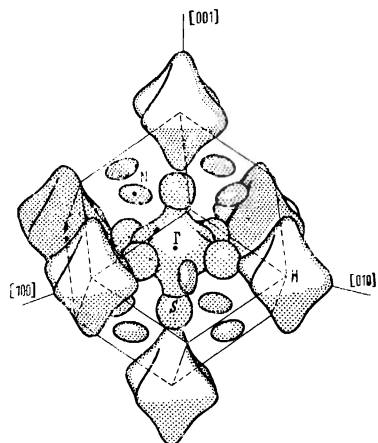


FIG. 1. Fermi surface of molybdenum and tungsten [16].

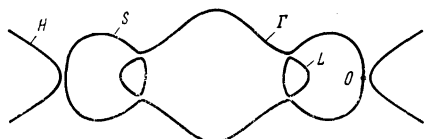


FIG. 2. Central section of the Fermi surface of molybdenum by the (110) plane. The section for tungsten is analogous, but the lenses L are missing there.

is the speed of light. To satisfy the condition $\nu + \nu_0 > \Omega$, it is necessary to carry out experiments on samples as thick as possible. The molybdenum samples were 0.52 and 0.38 mm thick, those of tungsten were 0.65 and 0.80 mm thick. The measurements were performed in a field H parallel to the sample surface, and during the temperature measurement we monitored the constancy of the shape and width of the lines.

The Fermi surfaces of tungsten and molybdenum are well known [13-15] (see Fig. 1). They consist of an electronic octahedron Γ , joined with six spheroids S , a hole octahedron H , and six hole ellipsoids N (for convenience we have designated these surfaces in practically all cases by the same letters as are used to designate the high-symmetry points of the Brillouin zone located at their centers). In addition, in molybdenum there are also six small electron lenses L (see Fig. 2). All the surfaces are closed, the summary volume of the hole surfaces is exactly equal to the volume of the electronic surfaces, and the total number of carriers is two per atom.

We have investigated the temperature dependences of eight lines in each of the metals; the orbits are indicated in Table I.

In molybdenum, the collision frequency in all cases turned out to be proportional to T^2 up to 12°K (see Fig. 3). The proportionality coefficient α , which we estimate to be accurate to about 10%, is apparently maximal on the neck between the Γ and S surfaces. This follows from the fact that the value of α for the orbit passing through the necks (see Fig. 2) turned out to be much larger than for the orbits that lie entirely on the Γ or S surfaces. A similar picture was obtained for copper, where the frequency of the collisions of the phonons with the electrons on the necks is 10 times larger than with the electrons on the central part of the surface [10]. Of course, the conclusion that strong scattering takes place on the necks is not unambiguous.

TABLE I

Surface	Direction of H	m/m_0	$v_i \cdot 10^{-4}$, cm/sec	$\alpha \cdot 10^{-7}$, $^{\circ}\text{K}^{-1} \cdot \text{sec}^{-1}$	$\beta \cdot 10^{-7}$, $^{\circ}\text{K}^{-1} \cdot \text{sec}^{-1}$	$\alpha' \cdot 10^{-7}$, $^{\circ}\text{K}^{-1} \cdot \text{sec}^{-1}$	$\beta' \cdot 10^{-7}$, $^{\circ}\text{K}^{-1} \cdot \text{sec}^{-1}$
Molybdenum, electronic surfaces							
Γ	[121]	1.38	0.6	1.6			
Γ	[111]	1.08		1.9			
$\Gamma-S$	[110]	2.50		2.9			
S	[110]	0.80		2.2			
Molybdenum, hole surfaces							
H	[121]	0.85	0.9	2.3			
H	[111]	0.80		2.1			
H	[110]	0.88		2.6			
N	[110]	0.40	0.8	3.6			
Tungsten, electronic surfaces							
Γ	[121]	0.88	0.7	4.9	0.47	1.8	0.03
Γ	[111]	0.83		4.7	0.48	1.4	0.05
$\Gamma-S$	[110]	1.83		2.0	0.29	0.8	0.22
S	[110]	0.56		2.1	0.28	1.3	0.14
Tungsten, hole surfaces							
H	[121]	0.63	1.2	4.4	0.12	1.4	0.02
H	[111]	0.57		4.0	0.10	0.50	0.06
H	[110]	0.67		4.5	0.16	0.3	0.14
N	[110]	0.27		0.6	4.2	0.95	

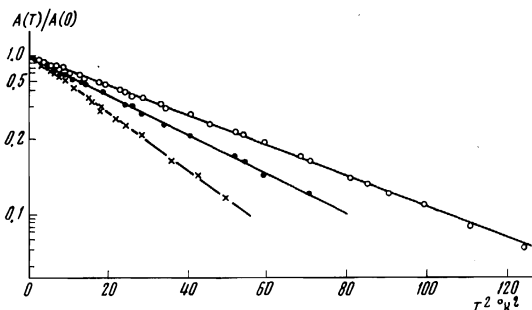


FIG. 3. Example of temperature dependence of the amplitudes of the size-effect lines for a molybdenum sample with thickness $d = 0.52$ mm; frequency $\omega/2\pi = 4.6$ MHz. \circ, \bullet - plots for lines from central surfaces H and Γ , respectively, at $H \parallel [111]$; \times - line from the section of the spheroid S at $H \parallel [110]$.

Generally speaking, the region of strong scattering can also be the vicinity of the point O on the spheroid (see Fig. 2).

It is more difficult to analyze the results for tungsten. In the entire temperature interval, the experimental points could not be described by either a quadratic or a cubic dependence on T (see Fig. 4). For all the investigated orbits, we obtained a relation $\nu = \alpha T^2$ at $T \lesssim 6^{\circ}\text{K}$ and the relation $\nu = \beta T^3$ at $T \geq 6^{\circ}\text{K}$. In addition to the quantities α and β , determined from diagrams of the type shown in Fig. 4, Table I also gives the results of a reduction of the experimental points by least squares in accordance with the formula $\nu = \alpha' T^2 + \beta' T^3$. This reduction presupposes the presence of two independent scattering mechanisms, by the electrons and by the phonons.

DISCUSSION

Since the dimensions [11,14] and the cyclotron masses [16-18] are known for all the individual sections of the Fermi surfaces, it is easy to obtain the mean values of the velocities v_i , which determine the density of states on each of the sections: $g_i = (4\pi^3 \hbar v_i)^{-1} S_i$ (S_i is the area of the corresponding section of the surface in k -space). As seen from Table I, the difference between the values of v_i is relatively small and gives no grounds for speaking of narrow trapping bands. This is also evidenced by data on the electronic specific

TABLE II. Density of states* and Debye temperature of tungsten and molybdenum and of certain nontransition metals from data on the specific heat [19]

	Metal															
	W	Mo	Li	Na	K	Cu	Ag	Be	Mg	Zn	Cd	Hg	Al	In	Sn	Pb
$10^{-34} G$	1.9	3.2	2.1	0.9	0.7	1.6	1.0	0.7	1.5	1.1	0.8	2.4	2.2	1.7	1.8	2.8
$\Theta, ^\circ K$	310	380	450	160	100	310	220	1030	330	240	220	90	390	130	170	90

*The density of states is given in $\text{erg}^{-1} \text{cm}^{-3}$.

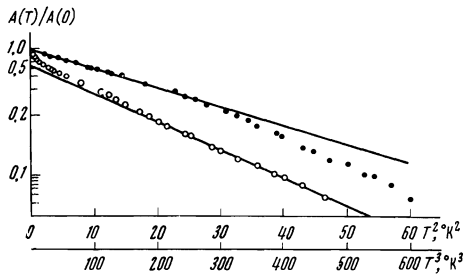


FIG. 4. Typical plots of the logarithm of the reduced size-effect lines for tungsten, plotted in the form of functions of T^2 (black circles) and T^3 (light circles); $d = 0.80 \text{ mm}$, $\omega/2\pi = 3.8 \text{ MHz}$, $H \parallel [110]$, orbit passes over the surfaces Γ and S (see Fig. 2).

heat [19]. The total density of states calculated from these data, $G = \sum g_i$, which is equal to $G_W = 1.9 \times 10^{34} \text{ erg}^{-1} \text{ cm}^{-3}$ for tungsten and $G_{Mo} = 3.2 \times 10^{34} \text{ erg}^{-1} \text{ cm}^{-3}$ for molybdenum, turns out to be of the same order as for nontransition metals (for example, for copper $G_{Cu} = 1.6 \times 10^{34} \text{ erg}^{-1} \text{ cm}^{-3}$, for aluminum $G_{Al} = 2.2 \times 10^{34} \text{ erg}^{-1} \text{ cm}^{-3}$, and for lead $G_{Pb} = 2.7 \times 10^{34} \text{ erg}^{-1} \text{ cm}^{-3}$) (see Table II).

When the contribution of the electron-electron collisions to the resistivity of transition metals is compared, for example, with that of alkali metals, reference is made to the different role played by the normal collisions. Inasmuch as in an alkali metal the attenuation of the current should be accompanied by dissipation of the momentum, the normal electron-electron collisions cannot make a contribution to the resistivity. The matrix element of the collisions with umklapp contains an additional interference factor, which is apparently quite small (see [20], Chaps. 4 and 9). On the other hand, if the carriers in the metal are both electrons and holes, then the current can be different from zero even at a zero total momentum of the system. Under these conditions, the collisions of the electrons with the holes, which are in essence normal collisions, contribute to the electric resistivity and the overall role of the electron-electron collisions should be appreciably larger.

The following remark can be made concerning this question. First, the normal but "interband" collisions should be significant not only in transition metals, but to an equal degree also, for example, in cadmium, zinc, or tin, where the number of electrons is equal to the number of holes. At the same time, the resistivity of these metals varies in accordance with the Bloch law. Second, one can refer to measurements made by the radio-frequency size effect, the line amplitudes in which are equally sensitive to all collisions, both normal and with umklapp. No quadratic term was observed in the collision frequency for any of the nontransition metals. (To be sure, the quadratic equation $\nu \propto T^2$ obtains in the

semimetals bismuth and antimony, but in their case there are weighty grounds for assuming that these are still collisions with phonons, and the unusual power T^2 in place of T^3 for the total collision frequency is due to the unique shape of the Fermi surfaces of semimetals [9].)

Thus, the difference between tungsten and molybdenum, on the one hand, and nontransition metals, on the other, does indeed call for a special explanation. The first explanation possibility, which is trivial to some degree, is that this difference can result from random numerical relations between two parameters, the Debye temperature Θ and the state density G . The first of them determines the frequency of the electron-phonon collisions $\nu_{ph} \sim \hbar^{-1} kT(T/\Theta)^2$, where K is Boltzmann's constant. (We have in mind the total frequency of the electron-phonon collisions. For electron-electron collisions, the difference between the total and transport frequencies is inessential, since the scattering is not at small angles.) The parameter G determines the frequency ν_e of the electron-electron collisions, inasmuch as the number n_2 of the scattered electrons and the number n_3 of the possible final states both increase with G : $n_2 \approx n_3 \approx kTG$ (for the detailed formulas see the Appendix).

It is thus possible in principle that the electron-electron collisions appear in tungsten and molybdenum as the result of the high Debye temperatures ($\Theta_W = 310^\circ K$, $\Theta_{Mo} = 380^\circ K$), which decreases the frequency of the collisions with the phonons. Indeed, as seen from Table II, for both tungsten and molybdenum the combination of values of G and Θ is quite favorable for electron-electron collisions, and more favorable for molybdenum than for tungsten. There are, however, counter arguments. For example, measurements have shown that in copper, in spite of the high Debye temperature, $\Theta_{Cu} = 310^\circ K$, we have $\nu \propto T^3$ on all sections of the Fermi surface, at any rate at $T \lesssim 3^\circ K$ [10].

From the point of view of ascertaining the role of the ratio of the parameters G and Θ , great interest attaches to aluminum, because both the density of states and the Debye temperature in it are higher than in tungsten. In the region of helium temperatures, the exponent in the $\rho(T)$ dependence of aluminum is undoubtedly smaller than 5 [21,22], but apparently the quadratic law is likewise not as well satisfied as for tungsten. In any case, there is no meeting of minds concerning the nature of the temperature dependence of the resistivity of aluminum at present. At the same time, no measurements of the collision frequencies for individual electron groups have made for aluminum as yet.

It is possible, besides, that there is some special reason that leads to the relation $\nu \propto T^2$ in transition metals, at any rate in tungsten and molybdenum. This reason should be sought not in the electronic spectrum itself, since the Fermi surfaces of these metals reveal no qualitative differences. The difference lies more readily in the genesis of the spectrum in transition and nontransition metals. In transition metals the spectrum is obtained in the approximation of weakly bound electrons, and the electronic ψ functions are almost unmodulated plane waves. In the case of the transition-metal spectra, the starting points are atomic ψ functions, and the calculation is carried out

in the strong-coupling approximation. Therefore the Bloch modulation factor $u(\mathbf{r})$ in the electronic ψ functions of the transition metals is strongly oscillating. This may turn out to be significant for the matrix elements of both the electron-electron and the electron-phonon scattering.

The authors are grateful to Yu. M. Kagan for valuable discussions and G. N. Landysheva for help with the measurements.

APPENDIX

Relations connecting the effective collision frequency measured in the size effect with the matrix element of the electron-phonon scattering were derived in ^[10]. We present here similar relations for electron-electron collisions.

Let us consider the scattering of an electron of energy ϵ_1 and wave vector \mathbf{k}_1 by an electron (ϵ_2, \mathbf{k}_2). Inasmuch as in the case of the anomalous skin effect the increment Δf for the distribution function differs from zero only along a narrow strip on the Fermi surface, it can be assumed that the distribution function f_2 of the scattering electron, and also the distribution functions f_3 and f_4 of the final states are in equilibrium: $f_i = [\exp(\epsilon_i - \epsilon_F)/kT + 1]^{-1}$, where ϵ_F is the Fermi energy. In the experiments one measures the rate of change of the quantity Δf due to the collisions. This change occurs both as a result of the change in the number of departures from the state \mathbf{k}_1 , and the change (as a result of the Pauli principle) of the number of arrivals at the state \mathbf{k}_1 from other states. The total change, normalized to one electron, is proportional to the function

$$\Phi(\epsilon_i) = f_2(1-f_3)(1-f_4) + f_3f_4(1-f_2) = f_2(1-f_3-f_4) + f_3f_4.$$

The total frequency ν_e for the scattering of the electron \mathbf{k}_1 is equal to the square of the matrix element of the interaction M_{12}^2 , multiplied by $\Phi(\epsilon_i)$, integrated over all the states of the scattering electron \mathbf{k}_2 and over all the final states \mathbf{k}_3 and \mathbf{k}_4 , with allowance for the energy and quasimomentum conservation laws. After making the change of variable $d^3\mathbf{k}_i = dS_i d\epsilon_i / \hbar v_i$ (dS_i is the equal-energy surface element and v_i is the electron velocity), the integration breaks up into two parts: "energy" and "geometrical." The integral over the energies can be calculated:

$$J(\epsilon_i) = \iiint \Phi(\epsilon_i) \delta(\epsilon_1 + \epsilon_2 - \epsilon_3 - \epsilon_4) d\epsilon_2 d\epsilon_3 d\epsilon_4 = \frac{(kT)^2}{2} \left[\pi^2 + \left(\frac{\epsilon_1 - \epsilon_F}{kT} \right)^2 \right]$$

and can be immediately averaged over the energy ϵ_1 of the electrons that enter in the increment Δf of the distribution function. Since $\Delta f \sim \partial f / \partial \epsilon$, we have

$$J = \int J(\epsilon) \frac{\partial f}{\partial \epsilon} d\epsilon \Big/ \int \frac{\partial f}{\partial \epsilon} d\epsilon = \frac{2}{3} \pi^2 (kT)^2.$$

The integral over the Fermi surface

$$I(\mathbf{k}_1) = \iiint (M_{12}^2)^2 \delta(\mathbf{k}_1 + \mathbf{k}_2 - \mathbf{k}_3 - \mathbf{k}_4 - \mathbf{K}) \frac{dS_2 dS_3 dS_4}{v_2 v_3 v_4}$$

(\mathbf{K} is the reciprocal-lattice vector) contains the form of the Fermi surface and the velocity distribution on the surface, as well as the matrix element of the interaction.

The Fermi-surface parameters of a number of transition metals can now be regarded as known. Therefore, if it is proved that the observed quadratic growth in experiments of the type described above is due to scattering by electrons, then it is possible in principle to obtain from such experiments more direct information on the electron-electron interaction than, for example, from data on the resistivity.

¹F. W. Ekin and B. W. Maxfield, Phys. Rev. B, **4**, 4215 (1971).

²R. N. Gurzhi and A. I. Kopeliovich, Zh. Eksp. Teor. Fiz. **61**, 2514 (1971) [Sov. Phys.-JETP **34**, 1345 (1972)].

³Yu. N. Kagan and A. P. Zhernov, ibid. **60**, 1832 (1971) [**33**, 990 (1971)].

⁴M. Ya. Azbel' and R. N. Gurzhi, ibid. **42**, 1632 (1962) [**15**, 1133 (1962)].

⁵D. K. Wagner, J. C. Garland, and R. Bowers, Phys. Rev. B, **3**, 3141 (1971).

⁶A. V. Vol'kenshtein, V. A. Novoselov, and V. E. Startsev, Zh. Eksp. Teor. Fiz. **60**, 1078 (1971) [Sov. Phys.-JETP **33**, 584 (1971)].

⁷L. D. Landau and I. Ya. Pomeranchuk, ibid. **7**, 379 (1937).

⁸N. F. Mott, Proc. Roy. Soc. (London) **A156**, 368 (1936).

⁹V. F. Gantmakher and V. T. Dolgoplov, Zh. Eksp. Teor. Fiz. **60**, 2260 (1971) [Sov. Phys.-JETP **33**, 1215 (1971)].

¹⁰V. F. Gantmakher and V. A. Gasparov, ibid. **64**, 1712 (1973) [**37**, 864 (1973)].

¹¹V. V. Boiko, V. A. Gasparov, and I. G. Gverdtsiteli, ibid. **56**, 489 (1969) [**29**, 267 (1969)].

¹²V. V. Boiko and V. A. Gasparov, ibid. **61**, 1976 (1971) [**34**, 1054 (1972)].

¹³T. L. Loucks, Phys. Rev. **139**, A1181 (1965); **143**, 506 (1966).

¹⁴V. V. Boiko and V. A. Gasparov, Zh. Eksp. Teor. Fiz. **61**, 2362 (1971) [Sov. Phys.-JETP **34**, 1266 (1972)].

¹⁵R. D. Girvan, A. V. Gold, and R. A. Phillips, J. Phys. Chem. Sol. **29**, 1485 (1968).

¹⁶W. M. Walsh, Jr., Solid State Physics **1**, Electrons in Metals, ed. F. P. Cochran and R. R. Haering, New York: Gordon and Breach, 1969.

¹⁷R. Herrmann, Phys. Stat. Sol. **25**, 427 (1968).

¹⁸R. Herrmann and H. Krüger, Phys. Stat. Sol. **41**, 99 (1970).

¹⁹K. A. Gschneidner, Sol. St. Phys. **16**, 275 (1964).

²⁰J. M. Ziman, Electrons and Phonons, Clarendon Press, 1960.

²¹F. C. Garland and R. Bowers, Phys. Kondens. Mat. **9**, 36 (1969).

²²F. R. Fickett, Cryogenics **11**, 239 (1971).

Translated by J. G. Adashko
123